International Journal of Applied Research 2021; 7(2): 474-477

ISSN Print: 2394-7500
ISSN Online: 2394-5869
Impact Factor: 8.4
IJAR 2021; 7(2): 474-477
www.allresearchjournal.com
Received: 11-12-2020
Accepted: 26-01-2021

Lal Prasad
Research Scholar,
Department of Physics,
L.N.M.U., Darbhanga, Bihar,
India

Correspondence Author:
Lal Prasad
Research Scholar,
Department of Physics,
L.N.M.U., Darbhanga, Bihar,
India

Study of the thermoelectric properties and electronic structures

Lal Prasad

Abstract
Electronic band structure calculations on $Cs_2BaCu_5Te_{10}$ at the density functional theory (DFT) level show a complex electronic structure near the Fermi level. In this paper, we study the two-dimensional structure of the compounds $A_2Bacu_5Te_{10}$ (A= k, Rb, Cs) fits the description of a "Phonon glass electron crystal" (PGEC) which good thermoelectric material. Electrical conductivity thermo power and thermal conductivity measured on polycrystalline ingots are reported, and the results are discussed in the conteret of the calculated electronic structure and the PGEC model.

Keywords: Thermoelectric properties, electronic structures, density functional theory

Introduction
There are several approaches to minimizing kı, the most intriguing is the one associated with the concept of "phonon glass electron crystal" (PGEC) which was introduced by Slack as the limiting characteristic for a superior thermoelectric. A PGEC material features cages (or tunnels) in its crystal structure inside which reside atoms small enough to "rattle"; i.e., create dynamic disorder. This situation produces a phonon damping effect which results in a reduction of the solid's lattice thermal conductivity. If the atomic orbitals of the "rattling" ions do not get substantially involved in the electronic structure near the Fermi level, the mobility of carriers is not likely to be substantially affected, thus not degrading potentially high electrical conductivity or thermopower.
Earlier, we reported on $A_2BaCu_8Te_{10}$ (A = K, Rb, Cs), a class of materials that possesses an anisotropic two-dimensional strucsture with Cu_8Te_{12} pentagonal dodecahedral cages.[4]In this sense these compounds are related to those of the clathrates, but formally they do not belong to this class. These cages are linked together to produce infinite $[BaCu_8Te_{10}]^{2-}$ slabs. The alkali metal ions are located between the slabs, and on the basis of their atomic displacement parameters (ADPs), undergo substantial thermal motion in the interslab space. It is interesting to note that the Ba^{2+} ions encapsulated in the Cu_8Te_{12} cages hardly undergo any "rattling" motion. It is the A^+ atoms that undergo such motion potentially scattering acoustic phonons. Because the structure of $A_2BaCu_8Te_{10}$ contains characteristics that fit the description for a PGEC candidate thermoelectric material, we decided to take a closer look at the thermal conductivity, its thermoelectric properties, and the details of its electronic band structure. The narrow energy gap in these materials was probed with a variety of experimental techniques such as heat capacity, magnetic susceptibility, and infrared absorption measurements. The results are discussed in the context of the electronic structure and the PGEC concept. Here, we demonstrate that the materials combine both low thermal conductivity and high electrical conductivity and therefore are viable for systematic thermoelectric investigations.

Analysis
Synthesis. Single crystals of $Rb_2BaCu_8Te_{10}$ and Cs_2BaCu_8- Te_{10} were obtained as described previously. Polycrystalline ingots of $Rb_2BaCu_8Te_{10}$ and $Cs_2BaCu_8Te_{10}$ were prepared with a different method described here for the first time. A polycrystalline powder was first synthesized by heating a mixture of Rb_2Te or Cs_2Te (1 mmol), BaTe (1 mmol), Cu (8 mmol), and Te (8 mmol) in a computer-controlled furnace to 520 °C in 12 h, isotherming at this temperature for 4-7 h, and quickly cooling to room temperature in 5 h. The polycrystalline

powder sample is then placed in a long silica tube with a diameter of 5 mm and flame sealed. The sealed tube is placed into a gentle flame to melt the compound and immediately quenched to liquid-nitrogen temperatures. This liquid-nitrogen quenching process helps avoid the formation of vacuum pockets inside the ingot. The $K_2BaCu_8Te_{10}$ can be prepared in a similar way.

Physical Measurements Electronic Transport Measurements

Ingot Samples. Polycrystalline ingot samples with typical sizes of 10 mm ×2 mm× 3 mm were cut from an ingot with a high-speed diamond saw. The ends of the samples were Ni plated and then were soldered to Cu blocks which had 0.003 in. Au-Fe (0.07 at. %) vs chromel thermocouples embedded in the Cu blocks to make the ΔT measurements. Cu lead wires were also soldered to these Cu blocks with one pair to serve as the current leads for the resistance measurements and another pair to serve as voltage leads (V_{TEP}) for the thermopower measurements. A pair of Au leads (V_R) were attached to the sample inside the current leads to measure the sample voltage for the resistance measurements. The sample voltages (V_{TEP} and V_R) as well as the thermocouple voltage (V_{TC}) were measured with a Keithley 2001 multivoltmeter. The Au-Fe vs chromel thermocouples provide adequate sensitivity even at the lower temperatures (T ‰ 4 K). The temperature of the sample is determined using a Lake Shore calibrated Cernox sensor. We performed standard four-probe resistance measurements on all our samples. The resistance of the sample was obtained by a dc method of reversing the current (Keithley 2400) at each temperature and measuring the sample voltage and then taking an average to subtract the thermal voltages. Typical sample currents were 5-50 mA. All data was taken using high-speed computer data acquisition software and instrumentation.

The thermopower was measured in two different ways. First a standard V_{TEP} vs ΔT curve was taken at several temperatures with the gradient on the sample being swept from -ΔT to + ΔT with ΔT = 2-5% of the absolute temperature, T. The slope was calculated and the Au lead contribution subtracted thus giving the absolute thermopower of the material. We use this method to check at several temperatures our more typical method. In the latter method, a ΔT of 2-5% T was established across the sample and the resistance and thermopower were measured at essentially the same time, as discussed above. The temperature of the sample was slowly lowered using a variable-temperature dewar from T ~ 300 K to T ~ 4 K over a period of 14-16 h, and the resistance and thermopower were monitored as a function of temperature.

Results and Discussion

Structure of A2BaCu8Te10: The structure type of $A_2BaCu_8Te_{10}$, the details of which have been described elsewhere, is two-dimensional with slabs of $[BaCu8Te10]^{2-}$ separated by layers of A^+ alkali metal cations; see Figure-1.

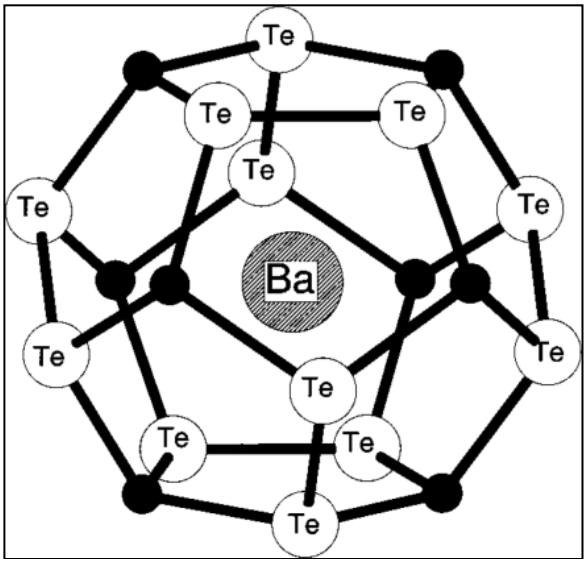

Fig 1: Ba-filled Cu_8Te_{12} cage of $Rb_2BaCu_8Te_{10}$.

The Cs salt on which the electronic structure calculation was made is orthorhombic *Immm* with a = 7.109(1) Å, b = 23.761(2) Å, and c = 6.966(1) Å. Depending on the identity of the alkali metal ion, the structure can adopt either a monoclinic or an orthorhombic cell, the difference between the two being the stacking of the $[BaCu_8Te_{10}]^{2-}$ layers. A strikingly characteristic feature in the structure is the Cu_8Te_{12} pentagonal dodecahedral cage, which incarcerates the Ba^{2+} ions; see Figure. Each cage cluster contains three mutually perpendicular sets of ditelluride units. The Cu_8Te_{12} cages form layers parallel to the (100) plane by sharing two pairs of oppositely spaced ditellurides along the *b*- and *c*-axis, respectively. The third and unshared Te_2^{2-} pair lines the surface of the Cu_8Te_{10} layer. The geometry around the Cu atom is slightly distorted tetrahedral.

Overall, the cage appears to have a strong affinity for cations with high charge/radius ratio, and so, given a choice between a Rb^+ and a $Ba2^+$ cation, it will encapsulate the latter. This preference is probably electrostatic in origin as the anionic layers of $[Cu_8Te_{10}]^{n-}$ attempt to reduce their negative charge. The bond distances between Cu and the Te_2^{2-} ligands range from 2.576(5) to 2.684(5) Å with an average of 2.64(5) Å. The Te-Te distances of the three ditellurides are in the range of 2.784(4) - 2.828(4) Å with an average of 2.80(2) Å. The Ba-Te distances inside the cage are almost independent of A^+ and average 3.75 Å. The

corresponding shortest A+-Te distances are 3.729(2) and 3.825(2) Å for Rb and Cs, respectively.

Electronic Structure Calculations

Unlike the $A_3Cu_8Te_{10}$ compounds, which possess mixed-valency and are good p-type metals [4] the $A_2BaCu_8Te_{10}$ compounds are electron-precise, as replacement of $Ba2^+$ for an alkali metal ion provides an additional electron to fill the hole in the valence band. As a result, they are expected to be semiconductors. Given the diffuse nature of the Te s and p orbitals, any band gap may be exceedingly small. To gain better insight into the nature of the band gap, we performed electronic structure calculations at the DFT level of theory.

The crystal structure has nine independent internal coordinates corresponding to the z-axis Cs position, the x-, y-, and z-axis Cu positions, the z-axis positions of Te(1) and Te(4), the y-axis position of Te(2), and the xand z-axis Te(3) positions. These were determined via total energy minimization using calculated atomic forces. The coordinates are given in Table 1 and remain remarkably close to the experimentally determined values. The Raman frequencies corresponding to these coordinates were determined by diagonalizing the dynamical matrix constructed from the calculated variation of the atomic forces. These are given in Table 2.

Table 1. Internal Structural Coordinates of $Cs_2BaCu_8Te_{10}$ Determined from First Principles Total Energy Minimization

	x	*y*	*z*
Cs	0.5	0.0	0.223
Ba	0.5	0.5	0.0
Te(1)	0.5	0.0	0.061
Te(2)	0.0	0.286	0.0
Te(3)	0.298	0.5	0.139
Te(4)	0.0	0.0	0.163
Cu	0.191	0.192	0.090

Table 2: Calculated Ag Symmetry Raman Active Phonons from First Principles Calculations

freq (cm^{-1})	polarization	main character
128	*x*	Cu
169	*x*	Te(3)
131	*y*	Te(2)
187	*y*	Cu
56	*z*	Cs, Te(3) (rattling mode)
69	*z*	Cs, Te(3) (rattling mode)
123	*z*	Te(4)
150	*z*	Te(1), Te(3), Te(4), Cu
171	*z*	Te(1), Cu

It is noteworthy that the lowest lying modes (softest) are those associated with the Cs+ atoms and they are expected at 56 and 69 cm^{-1}. The low-frequency, mixed character of these modes is consistent with the "rattling" ion scenario for obtaining glasslike thermal conductivity. Unfortunately, we were unable to probe Raman frequencies below 90 cm^{-1} with our experimental apparatus. Perhaps quasi-elastic neutron scattering could be of help here to observe and identify these very soft modes.

The band structure along selected symmetry directions is shown in Figure 2.

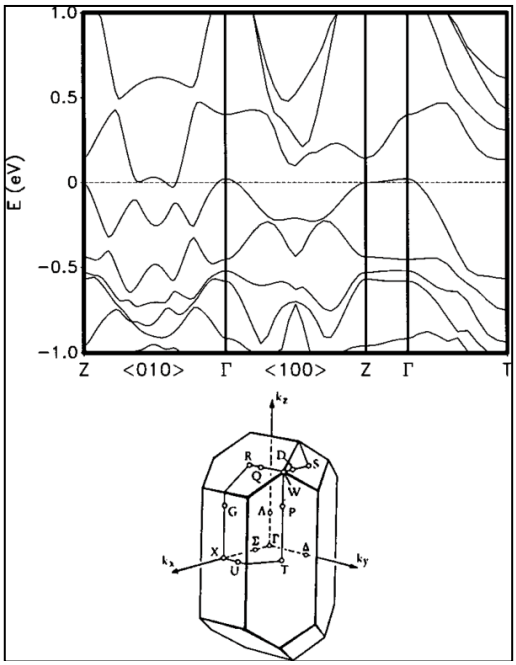

Fig 2: Band structure of $Cs_2BaCu_8Te_{10}$ along selected directions in the body centered orthorhombic Brillouin zone. EF is denoted by the dashed horizontal line at 0 eV.

Assuming that a very small gap actually exists, it is evident from Figure 4 that it is indirect. The top of the valence band occurs at the Γ and Z points (<100> direction), whereas the bottom of the conduction band occurs in several places in the Brillouin zone away from the zone boundaries. There are two optical thresholds expected from the band structure. The first involves transitions between the lower and upper band edges from the anti-crossing states; the second is the gap at the Z point, calculated as 0.20 eV.

The hole cylinder around Γ is derived from well hybridized Te p and Cu d states and may be expected to have reasonable carrier mobility for transport in the *ab*-crystallographic plane. There is very little dispersion along the *c*-axis (*Z*) direction, and so this component of the resistivity should be much higher. In fact *c*-axis transport may well be incoherent at room temperature. The effective mass tensor of the whole cylinder at Γ has *x*- and *y*-components of 0.78 and 0.41 *m*e, respectively. This implies significant anisotropy of the transport properties in the *ab*-plane as well. In the simplest, constant scattering kinetic transport theory, the *b*-axis conductivity of p-type samples, where this band dominates, would be 3.6 times larger than in the *a*-axis direction. This is the direction of the Te_2^{2-} bonds which cover both sides of the $[BaCu_8Te_{10}]$ layers.

The electron states (n-type doping) derive from a band dominated by Te p orbitals, which dips down toward *E*F at the nominal simple orthorhombic zone boundary. This corresponds to the midpoints of the basal plane <010> and <100> Γ -*Z* directions in the body-centered zone as shown in Figure 2. Along <100> this band just "kisses" *E*F, while along <010> the dispersion is slightly larger so that it crosses *E*F descending to -0.3 eV. However, there is an anticrossing with a hybridized band dispersing upward from Γ along this line to 0.05 eV above *E*F at the midpoint (nominal zone boundary). The anticrossing opens a gap around *E*F and mixes the character of these two bands. The resulting electron pockets have a complex shape and, like the hole cylinder, are considerably less dispersive in the *c*-axis direction as compared with the *ab*-plane.

We note that the band structure of the isostructural $Cs_3Cu_8Te_{10}$ around *E*F is very similar and shows the same features, except that the electron count is reduced by one, so that *E*F lies below rather than above the gap produced by the anticrossing. The main difference around *E*F is an upward shift of a little more than 0.2 eV of the anticrossing relative to the band comprising the hole cylinder. This rigid band property has implications for the charge transport. In particular, it suggests that Cs impurities on the $Ba2^+$ site of $Cs_2BaCu_8Te_{10}$ should be effective p-type dopants providing carriers but with little scattering. Also, soft phonons that may be associated with A^+ (Rb, Cs) atom vibrations will show moderately weak electron-phonon interactions, implying low thermal conductivity but reasonably high hole mobility in these materials.

Conclusion

The $A_2BaCu_8Te_{10}$ phases are narrow gap semiconductors with very low thermal conductivity. However, the heat conduction in these materials seems to be frustrated mainly by factors such as low crystal symmetry and possibly mass fluctuation disorder between alkali (i.e. Cs case) ions and Ba ions in the structure and less by soft rattling modes of the alkali A+ atoms between the layers. The moderately high room-temperature conductivity of these compounds, coupled with their relatively high thermo-power values and very low thermal conductivity, raises the possibility that they may be valuable for thermoelectric.

References

1. Thermoelectric Materials. The Next Generation Materials for Small-Scale Refrigeration and Power Generation Applications; Material Research Society Symposium Proceedings, 1998, 545.
2. Tritt TM, Kanatzidis MG, Mahan GD, Lyon HB. Eds.; MRS: Pittsburgh, PA, 1988.
3. Tritt TM, Kanatzidis MG, Lyon HB, Mahan GD. Eds.; MRS: Pittsburgh, PA. Thermoelectric Materials-New Directions and Approaches; Material Research Society Symposium Proceedings, 1997, 478.
4. Chung DY, Iordanidis L, Choi KS, Kanatzidis MG Bull. Kor. Chem. Soc. 1998;19:1283-1293.
5. Kanatzidis MG, DiSalvo FJ. Thermoelectric Materials: Solid State Synthesis. Naval Res. Rev. 1996;68(4):14.
6. Kanatzidis MG. In Semiconductors and Semimetals; Tritt, T., Ed.; Academic Press: New York, 2000.
7. Slack GA. New Materials and Performance Limits for Thermoelectric Cooling. In CRC Handbook of Thermoelectrics; Rowe DM. Ed CRC Press: Boca Raton, FL, 1995, 407-440.
8. Slack GA. In Thermoelectric Materials-New Directions and Approaches; Material Research Society Symposium Proceedings. Tritt TM, Kanatzidis MG, Lyon HB, Mahan GD, Eds.; MRS: Pittsburgh, PA, 1997, 47.